Location Related Signals with Satellite Image Fusion Method Using Visual Image Integration Method

Dr. G. Ravikanth[1]**, Dr. K. V. N. Sunitha**[2†] **and Dr. B. Eswara Reddy**[3]

[1] *Professor, BVC College of Engineering, Palacharla, Rajahmundry, Andhra Pradesh, India*
[2] *Professor & Principal, BVRIT Hyderabad college of Engineering for Women, Bachupally, Hyderabad, Telangana-India*
[3] *Professor & Director, Software Development Centre, JNT University, Ananthapuramu, Andhra Pradesh, India*

Investigations were performed on a group utilizing (General Purpose Unit) GPU and executions were evaluated for the utilization of the created parallel usages to process satellite pictures from satellite Landsat7.The usage on a realistic group gives execution change from 2 to 18 times. The nature of the considered techniques was assessed by relative dimensionless global error in synthesis (ERGAS) and Quality Without Reference (QNR) measurements. The outcomes demonstrate execution picks ups and holding of value with the bunch of GPU contrasted with the outcomes and different analysts for a CPU and single GPU. The errand of upgrading the view of a scene by combining data caught from various picture sensors is usually known as multisensor picture combination. This paper displays a territory based picture combination calculation to consolidate SAR (Synthetic Aperture Radar) and optical pictures. The co-enlistment of the two images is first led utilizing the proposed enrollment method prior to picture combination. The paper displays a parallel execution of existing picture combination techniques on a graphical group. Parallel executions of techniques in view of discrete wavelet changes are created. Division into dynamic and motionless regions is then executed on the SAR surface picture for particular injection of the SAR picture into panchromatic (PAN) picture. An integrated image in view of these two pictures is produced by the novel region based combination plot, which forces diverse combination rules for each fragmented region. At long last, this picture is melded into a multispectral(MS) picture through the half breed skillet honing technique proposed in past research. Exploratory outcomes exhibit that the proposed strategy demonstrates preferred execution over different fusion algorithms and can possibly be connected to the multisensory combination of SAR and optical pictures.

Keywords: Area-based combination conspire, co-enlistment, hybrid sharpening, multisensor picture combination, wavelet change., Image combination, Cluster, GPU, Wavelet, Satellite.

1. INTRODUCTION

Remote detecting is a procedure of social occurrence data about the question, region or marvel without coordinate contact. Techniques for remote detecting established on simple or computerized enrollment in light of electromagnetic outflows from objects or on reflected waves over a wide otherworldly range. The results of remote detecting are computerized pictures with pixel esteems relating to the value(s) of properties, in separate zones. The measure of the zone relies upon the determination of the pictures.

With the current, quick advancements in the field of detecting innovations, multi sensor imaging frameworks are being utilized as a part of a developing number of fields, for example, in remote detecting and military applications. Multi sensor picture combination, which is characterized as the way toward joining significant data from at least two pictures into a solitary picture, has been getting expanding consideration in the remote detecting

*garladinne.ravikanth@gmail.com
†k.v.n.sunitha@gmail.com

research group because of the expanding accessibility. Melded pictures ought to be more helpful for additionally picture handling assignments, for example, picture division, protest distinguishing proof, and provincial change location [3]–[6]. This sort of picture combination is likewise called pixel-level multisensory picture combination [2].

Different multi sensor picture combination plans have been developed over the previous couple of years. A relative assessment of ten combination systems for testing the viability of combination TerraSAR-X and SPOT 5 pictures are portrayed in [7]. It is demonstrated that the Ehlers combination technique, which depends on a force tone immersion (IHS) change combined with Fourier space sifting, is more effective for multi sensor picture combination than other combination strategies. A multisensor picture combination calculation in light of power tweak was proposed by Alparone et al. [8] for incorporating PAN and SAR highlights into MS pictures; it depends on SAR surface removed by rationing the despeckled SAR picture to its low-pass guess with "à trous" wavelet decay. It can change the measure of incorporation utilizing an edge to stay away from full reconciliation of SAR highlights.

2. RELATED WORK

Most satellites, for example, SPOT, IRS, Landsat 7, IKONOS, Quick Bird, Orb View, and sensors, for example, the Leica ADS40, give panchromatic pictures high determination and multispectral with low determination [1]. A compelling technique for combining pictures may extend the utilization of such pictures in numerous regions that require high otherworldly and spatial picture determination all the while [20]. In this manner, the errand of consolidating remote detecting comes about is the incorporation of geometric subtle elements from panchromatic (PAN) picture with a high determination and shading data contained in multispectral (MS) picture with a lower determination (for instance in geo-data frameworks) [2].

Since 80's of the 20th century was created various techniques for picture combination for remote detecting issues [3,4]. This work is identified with picture combination for remote detecting and has the principle objective of enhancing efficiency of picture combination process. As of late, Graphics Processing Units (GPUs) are generally utilized for superior registering, including picture combination [5,6].

Graphical bunch is an appropriated parallel figuring framework with hubs supporting broadly useful processing, furnished with video cards [21]. This paper depicts the usage strategies for picture combination utilizing a bunch of GPU.

In thickly populated urban situations specifically, where numerous substantial structures of different shapes and complex rooftop structures are found near one another, the radar backscatter reactions are very high, and the spatial examples of the backscatter are likewise sporadic on the grounds that structures frequently go about as curve reflectors to radar flag and diffusing systems from nearby structures are very confounded [7]. The backscatter forces of most thickly populated urban zones in SAR pictures in this manner have heterogeneous qualities, aside from a few regions where low-ascent structures with level rooftops are detached from encompassing structures

and different structures [22]. These heterogeneous qualities negatively affect the interpretability of these territories in the melded picture in view of ghostly mutilation coming about because of the generous divergence between the SAR picture and the optical picture [23].

3. PROPOSED METHOD

The decision of picture combination technique:

Systems of picture combination can be separated into such classes: added substance and multiplicative techniques and strategies in light of channels or the connections between the channels and changes, for example, the discrete wavelet change (DWT) [7,8].

DWT-technique in light of supplanting the coefficients of the approximations with the information from multispectral channel was picked as a fundamental strategy for the parallel execution [24]. The decision of this strategy is grounded by exclusive standards of measurements estimation of the combination quality. Fig. 1 demonstrates the clarification of this technique.

Proportion of the channels measure (PAN and MS) is thought to be 4/1. The strategy contains these means:

- Direct 2D DWT of the PAN channel.

- Replacement of coefficients of the estimation by the multispectral information channel.

- Inverse 2D DWT.

The 2D change is performed by applying a one-dimensional change to the lines of the grid speaking to the picture and afterward to the sections. Essentially, two-dimensional converse change is performed by applying a switch one-dimensional change to the segments and afterward to the columns of the framework.

The paper demonstrates the usage of two strategies in view of DWT– Haar and Daubechie techniques [9,10]. The direct 1D discrete wavelet Haar change is performed by Eq.(1)–(2):

$$t'_i = (\tau_{2i} + t_{2i+1})/2 \tag{1}$$

$$t'_{N/2+i} = (t_{2i} + t_{2i+1})/2 \tag{2}$$

Where $i \in [0, N/2]$, s_i is the component of the input vector, s'_i is the component of the output vector, and N is the vector length. The direct 1D discrete wavelet Daubechies transform is performed by Eq. (3)–(6):

$$t'_i = \sum t_{2i+k} h_k \tag{3}$$

$$t'_{N/2+i} = \sum t_{2i+k} g_k \tag{4}$$

$$t'_{N/2-1} = \sum t_{N-2+m} h_m + \sum t_m h_{2+m} \tag{5}$$

$$t'_{N-1} = \sum t_{N-2+m} g_m + \sum t_m g_{2+m} \tag{6}$$

where $I \in 0, N/2 - -1$, $k \in 0, 3$, $m \in 0, 1$, s_i is the component of the input vector, s'_i is the component of the output vector, N is the vector length, and h and g are calculated by Eq. (7)–(10):
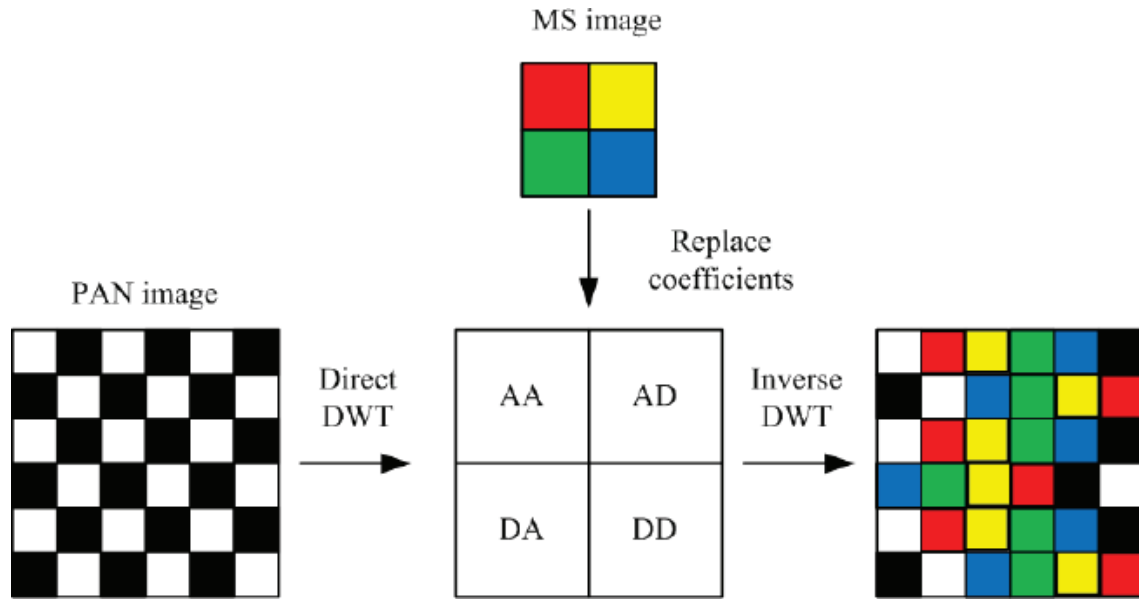
Figure 1 DWT-based methods explanation.

$$h_i = (1 + 2i + \sqrt{3})/4\sqrt{2} \qquad (7)$$

$$h_{i+2} = (3 - 2i - \sqrt{3})/4\sqrt{2} \qquad (8)$$

$$g_i = (2i + \sqrt{3} - 3)/4\sqrt{2} \qquad (9)$$

$$g_{i+2} = (\sqrt{3} - 1 - 2i)/4\sqrt{2} \qquad (10)$$

where $i \in [0, 1]$. The inverse 1D discrete wavelet Haar transform is performed by Eq. (11)–(12):

$$t_{2i} = t'_i + t'_{N/2+i} \qquad (11)$$

$$t_{2i+1} = t'_i - t'_{N/2+i} \qquad (12)$$

where $i \in [0, N/2)$. The inverse 1D discrete wavelet Daubechies transform is performed by Eq. (13)–(16):

$$t_0 = \sum t'_{N/2-1+k} S_{3k} + \sum t'_{(N-1)k} S_{2-k} \qquad (13)$$

$$t_1 = \sum t'_{N/2-1+k} v_{3k} + \sum t'_{(N-1)k} v_{2-k} \qquad (14)$$

$$t_{2+2i} = \sum t'_{i+k} S_{2k} + \sum t'_{i+N/2+k} S_{1+2k} \qquad (15)$$

$$t_{3+2i} = \sum t'_{i+k} v_{2k} + \sum t'_{i+N/2+k} v_{1+2k} \qquad (16)$$

where $i \in [0, N/2 - -1]$, $k \in [0, 1]$, and t and u are calculated as $t0 = h2$, $t1 = g2$, $t2 = h0$, $t3 = g0$, $u0 = h3$, $u1 = g3$, $u2 = h1$, $u3 = g1$. ui , giare obtained using Eq. (7)–(10).

3.1 Process implementation on equivalent system:

Accepting that the aftereffect of the combination of parts took after by an association is identical to combination of the first informational index all in all, can offer a plan for errand division on the bunch hubs [25] [26]. The source network is part on a level plane and vertically into a balance of, each part is then handled on a different hub in the bunch and the last outcomes converge into a solitary picture on the ace hub. Each group hub performs picture

handling, pixel by pixel, utilizing two-dimensional exhibit of strings. A schematic of the dividing procedure is appeared in Fig. 2. Fig. 3 demonstrates a flowchart of the parallel calculation for multispectral combination.

To sort out the correspondence between hubs in the group, MPI execution from Argonne National Laboratory - MPICH2 was utilized [11]. Picture preparing on every hub is performed utilizing General-Purpose Computing on Graphics Processing Unit (GPGPU) card with a Compute Unified Device Architecture (CUDA) innovation [5].

With a specific end goal to quicken the way toward exchanging information between hubs, pictures are moved in to the portrayal of 8 bpp. In any case, at a combination, the procedures are performed utilizing the gliding point single exactness portrayal of 32 bpp which is essential for the discrete wavelet change.

The combination procedure on the GPGPU card comprises of the accompanying strides for each channel:

- stack PAN divert in the main piece in surface memory;

- assign a cluster in worldwide memory for the PAN channel;

- stack MS direct in the second square in surface memory;

- perform coordinate 1D DWT over the columns of PAN exhibit with perusing information from surface first square and composing into the worldwide cluster;

- duplicate pixels from worldwide exhibit to surface first piece;

- perform coordinate 1D DWT over the sections PAN cluster with perusing information from surface first piece and composing into worldwide exhibit;

- supplant the coefficients of estimate in worldwide cluster with MS coefficients from texture second square;

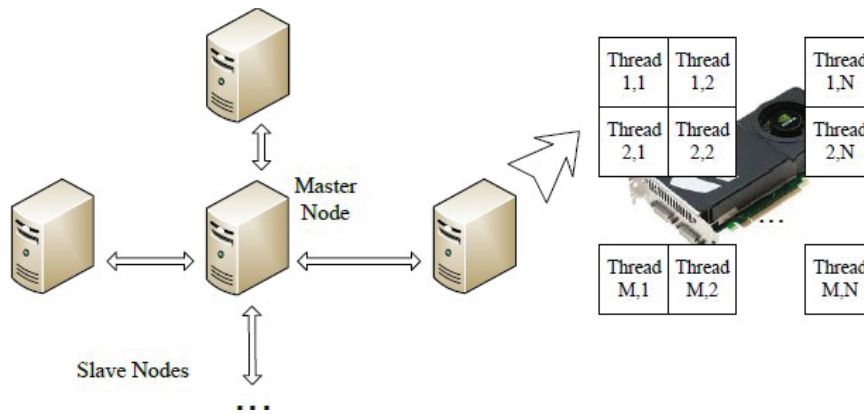- duplicate worldwide cluster to surface first piece;
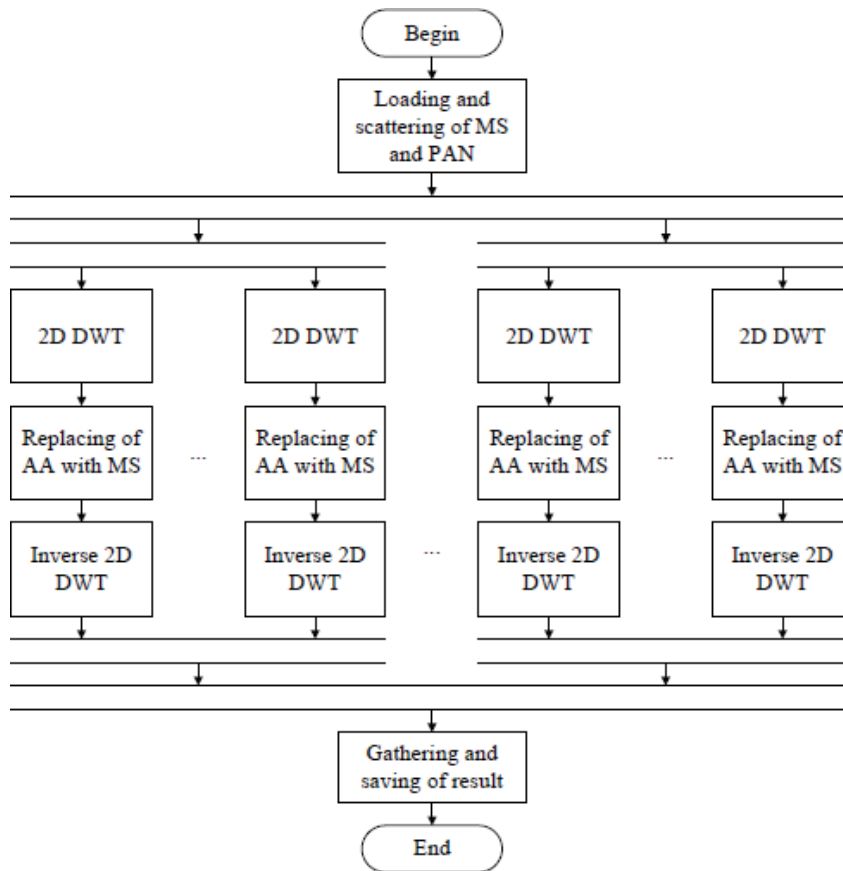
Figure 2 Clusters Model

Figure 3 Flowchart of parallel algorithm for multispectral image fusion.

- perform backwards 1D DWT over segments perusing from surface first piece and composing into the worldwide cluster;

- duplicate worldwide cluster to surface first piece;

- perform reverse 1D DWT over lines perusing from surface first square and composing into the worldwide exhibit;

- empty the outcome from worldwide exhibit.

For this situation, it is required to accomplish an elite through the perusing from surfaces' memory and consecutive written work into the worldwide memory and duplicating information between parts of gadgets without utilizing a brief memory.

3.2 Image Fusion Algorithm

In this paper, we melded the first MS, PAN and SAR pictures utilizing the half and half container honing calculation. In the half breed skillet honing calculation, a PAN picture is reserved with a PS picture, which implies the coordination information for PAN and SAR pictures are controlled by (11). Let be the combined picture of the nth with high spatial determination and be the multispectral picture. The over all technique is portrayed in (13).

$$P_n^h = NT_n^l + \lambda_n \cdot \left[\mu_n \cdot F_n + u_n \cdot \text{Lap}\,(F_n) \right]$$

Where λn is the underlying combination parameter of the nth band,Hn is the essential high-recurrence data, Lap(.)means the Laplacian picture sifting, and μn and vn are the alteration coefficients, separately. Parameters utilized as a part of (13) are characterized as underneath [12], [13].

$$F_n = UT_n^h - I_n^l$$

$$\lambda_{n(x,y)} = T_n \times \sqrt{\frac{\sigma\left(NT_{n(x,y)}^l\right)}{\sigma\left(I_{n(x,y)}^l\right)} \times T_{n(x,y)}}$$

$$\mu_n = \max\left(\frac{\sigma\left(NT_n^l\right)}{\sigma\left(I^l\right)}, \frac{\sigma\left(I^l\right)}{\sigma\left(NT_n^l\right)}\right),$$

$$if \frac{\sum_{n=1}^N \frac{i}{N} \text{Ent}\left(NT_n^l\right)}{\text{Ent}\left(I^l\right)} \leq thr$$

$$= \frac{\sigma\left(I^l\right)}{\sigma\left(NT_n^l\right)}, \text{ if } \frac{\sum_{n=1}^N \frac{i}{N} \text{Ent}\left(NT_n^l\right)}{\text{Ent}\left(I^l\right)} > thr$$

$$u_n = \frac{\sigma\left(F_n\right)}{2.\sigma\left(F_n'\right)}$$

where PAN is the histogram-coordinated incorporated picture of PAN and SAR pictures given in (11), Ilt is the force picture by relapse between and PSh, implies the balanced power picture. furthermore, acquired by Laplacian sifting, and σ (.)is the standard deviation. In (16), the nearby estimation of λ $n(x, y)$ at (x, y) can be figured by a moving window. At that point, it depends on the neighborhood connection co-proficient $Sn(x, y)$. Notwithstanding, a circled bend molded edge happens λn(x, y) in the as a result of numerical hazards. Then, the half and half calculation is advanced to optical dish honing of MS and PAN pictures. What's more, spatial and phantom attributes of joining information for PAN and SAR pictures might be not the same as those of an optical PAN picture. In this way, we amended (15) with a specific end goal to think about the measure of spatial data in the joining information and to upgrade the infusion part of spatial and ghostly data into the incorporation information. The overhauled condition is characterized as (18).

$$\lambda_{n(x,y)} = \frac{T_n}{\omega_1} \times \sqrt{\frac{\sigma\left(NT_{n(x,y)}^l\right)}{\sigma\left(I_{n(x,y)}^l\right)} \times T_{n(x,y)}}$$

where ω1 is the relating weight coefficients that utilized the coordination of PAN and SAR pictures. At the point when joining information incorporates a greater number of qualities of SAR pictures than of PAN pictures, or the information incorporates non-urban territories more than urban zones.

4. RESULT:

To give the premise to looking at the quality and execution of strategies, two different techniques for usage have been picked: a weighted averaging strategy and a technique in view of the change of shading space (IHS) [7,8]. Likewise, for every single actualized strategy, measurements have been gotten for the bunch of CPUs.

For the examinations on genuine information benefit USGS Global Visualization Viewer from

U. S. Geographical Survey were utilized. To get appraisals of profitability and quality, symbolism were chosen, from satellite Landsat 7 [12], which are zone photos of the Donetsk district (Ukraine).

In table 1and 2 are utilized taken after abbreviators:

- WA – weighted averaging technique;

- IHS – Intensity Hue Saturation technique;

- HDWT – Haar discrete wavelet change;

- DDWT – Daubechies discrete wavelet change.

As takes after from Table 1, the execution of the IHS strategy has the best time on group with GPU. This is on account of the GPU direction set is more productive for execution of IHS.

As takes after from Table 2, the execution of the HDWT strategy has the best time on group with CPU. This is on the grounds that this usage, proficiently actualized utilizing number-crunching tasks of CPU, does not utilize picture scaling and discrete wavelet change.

Since the objective of this work was to enhance the execution of parallel usage, we ought to decide how to gauge the execution. For this situation, the yield will be the quantity of tasks every second, while activities with memory and accepting that all tasks are by and large equivalent in intricacy.

Fig. 4 demonstrates the examination of development execution for every strategy among usage on realistic group and bunch of CPU. In light of examination of Fig. 4, we can infer that the execution pick up of parallel usage on GPU lies in the range 2–18 times relying upon the combination strategy. With a specific end goal to outline and obviously separate among the thought about techniques, Fig. 5 indicates four pictures that are the consequences of every one of the actualized strategies.

The measurements ERGAS (Error Global in Synthesis) and QNR (Quality Non Reference) are utilized for assessing the nature of the thought about strategies (Table 3).

As takes after from Table 3, the HDWT technique has the best quality (littlest blunder for ERGAS, and the most noteworthy quality for QNR), that reliably concurs with the subjective visual appraisal of the outcome pictures of Fig. 5. It ought to be noticed that measurements for DDWT technique don't meet the normal outcomes. In view of hypothetical suppositions, the DDWT strategy ought to give an exceptionally nitty gritty picture which is related with excellent measurements (QNR). Yet, the aftereffects of the examination demonstrate that the DDWT has a negative QNR. This might be clarified by "finished infusion" and subsequently we have negative QNR (spatial quality record is higher than the unearthly so their distinction is negative).

An execution pick up in the scope could be contrasted with comparable outcomes that were acquired in [13]. In that reference, the creators acquired 10% expansion in the execution utilizing GPU contrasted with utilizing CPU. They utilized single GPU GTX 550Ti. This exploration demonstrates that the GPU group even with a less intense processor GTX 460 could work in 2–18 times speedier with a similar picture measure.

In this paper, we utilized satellite pictures from IKONOS, KOMPSAT-2, and TerraSAR-X to confirm the nature of combined picture produced by our calculation. Before picture

Table 1 GPU cluster.

PAN width,px	PAN height,px	T_{WA},sec	T_{HS},sec	T_{HDWT},sec	T_{DDWT},sec
16280	14960	3,73	3,01	3,61	3,70
8140	7480	0,90	0,85	0,98	1,02
4070	3736	0.32	0,30	0,34	0,35

Table 2 Quality constraints comparision.

Metric	WA	HIS	HDWT	DDWT
QNR	0.35	0.30	0.42	−0.10
EGRAS	50.85	42.98	27.43	79.84

Table 3 Fusion of images result analysis.

| Dataset	Index	Hybrid Pansharpening (PAN only)	WC	MR	MBT-CW	Proposed method
KOMPSAT-2 Vs TerraSAR-X	RASE	3.055	6.402	5.111	8.193	3.087
	ERGAS	1.573	2.385	1.309	2.008	0.858
	SAM	1.511	1.562	0.559	0.455	0.713
	Q_{avg}	1.950	1.484	0.501	0.814	0.907
	D_λ	1.052	1.499	0.487	0.206	0.098
	sCC	1.891	1.980	0.865	0.203	0.874
	AG	12.469	11.559	11.175	37.573	23.301
IKONOS Vs TerraSAR-X	RASE	13.051	1.730	29.094	28.347	14.166
	ERGAS	3.903	8.852	7.390	6.750	3.162
	SAM	1.158	2.492	2.911	2.049	2.942
	Q_{avg}	1.896	1.048	0.569	0.801	0.879
	D_λ	1.110	1.759	0.505	0.211	0.135
	sCC	1.975	1.991	0.991	0.497	0.967
	AG	126.694	92.747	97.561	161.869	229.312
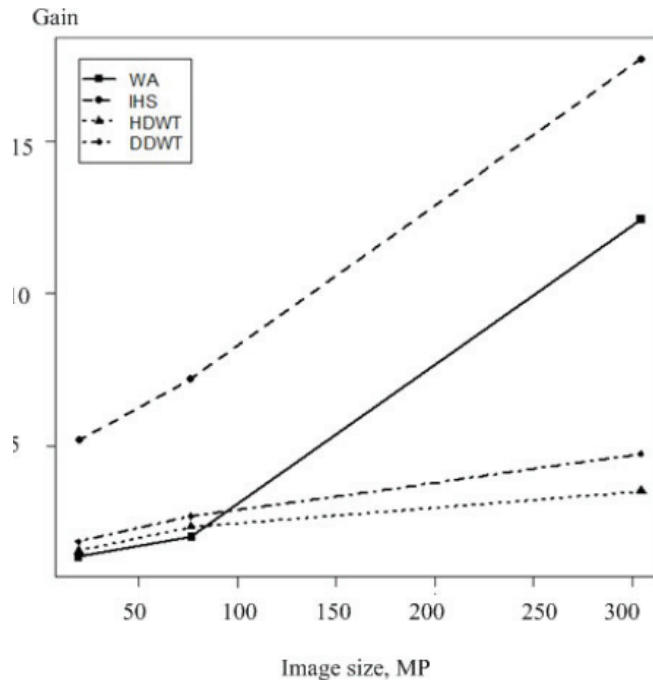
Figure 4 Performance improvement of cluster with GPU compared to the cluster of CPU.

combination, the TerraSAR-X picture was scaled from 18 bits to 9 bits to dispense with information repetition, and the MS pictures of each dataset were resampled so they Would have an indistinguishable spatial determination from the PAN and SAR pictures.

Contrasting the first dish honing result and our reconciliation result, the lower ghostly lists demonstrates an unavoidable distinction because of the infusion of extra data from the SAR picture, including dissimilarities from the MS and PAN pictures. Figure 6 represents the analysis of PAN images and Figure 7

Figure 5 Result of image fusion (from left to right and from top to bottom - WA, IHS, HDWT, and DDWT).
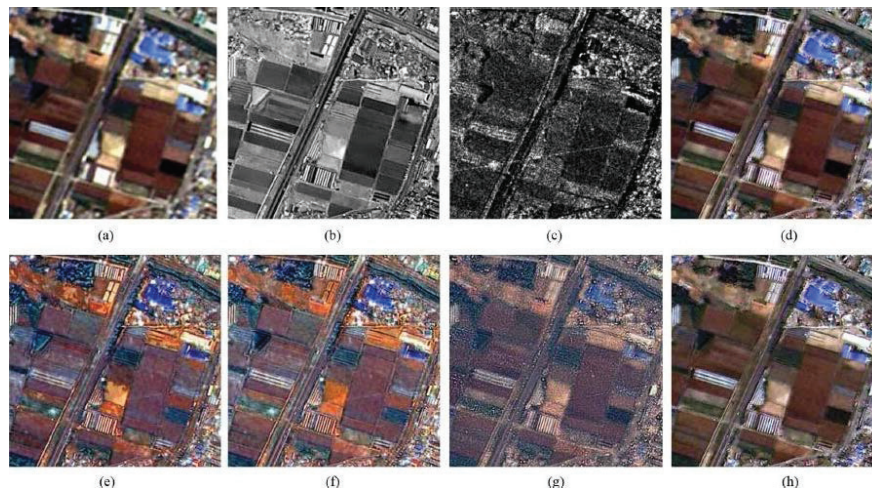

Figure 6 Analysis of PAN images with Result.

depicts the analysis of SAR images. In this manner, our multisensory combination calculation can safeguard the vast majority of the other worldly data from unique MS pictures in melded pictures by including attributes of the SAR information however much as could reasonably be expected. What's more, our calculation yields a superior AG esteem than different techniques, except for the MBT-CW strategy. In any case, MBT-CW offers less conceivable outcomes for spatial understanding than our calculation due to the exorbitant infusion of spot pixels or commotion into the PAN picture. The intertwined picture acquired utilizing our calculation has a higher CC esteem than the MBT-CW strategy.

5. CONCLUSION

The paper displays a parallel usage of existing strategies for combination of pictures on the design of a realistic group. Trial aftereffects of testing of parallel executions demonstrate that the IHS technique has the best outcome on a group of CPU and the HDWT strategy has the best outcome on a bunch of GPU. The usage on a realistic group gives execution change from 2–18 times. The proposed parallel execution utilized for picture combination in a product framework for preparing remote detecting information from satellite. In this paper, another technique is proposed for multi sensor picture combination
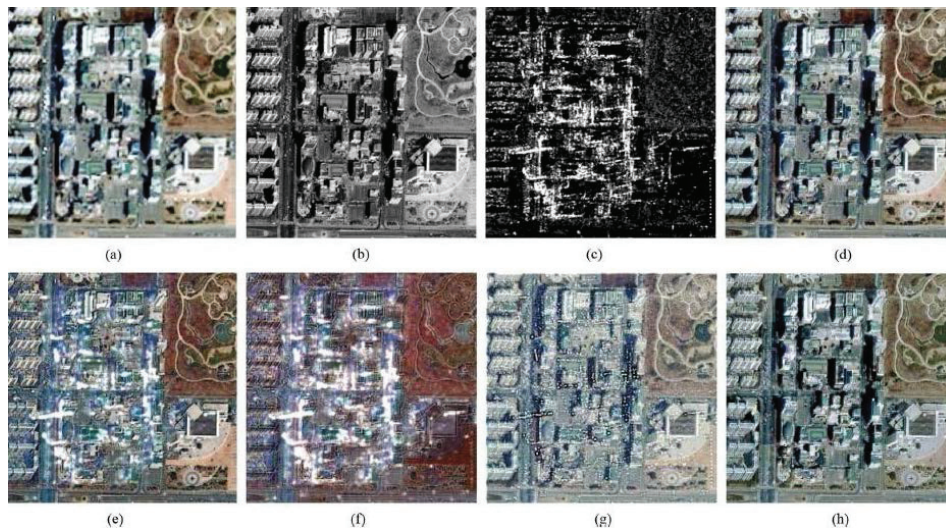
Figure 7 Analysis of SAR images with result.

where a region based combination run was utilized to address the combination of optical and SAR pictures. At initially, division into dynamic and dormant zones is performed utilizing SAR surface data. The latent regions are melded utilizing just PAN pictures, and the dynamic territories are intertwined utilizing the pixel-based weighted blend of PAN and SAR pictures. Taking everything into account, by joining just the SAR highlights of dynamic (homogeneous) regions into optical pictures, we can effectively expand the interpretability of the combined picture. To analyze execution, our calculation is assessed both by visual and quantitative strategies and contrasted and different other combination calculations. The appraisals demonstrate that the proposed strategy is more adaptable than alternate techniques, since it can give data on particular combination that contemplates territorial qualities. Future work will center around mapping and elucidation utilizing pictures upgraded by the combination of SAR and optical pictures contrasted with those of isolated SAR or optical pictures.

REFERENCES

1. C. K. Munechika, J. S.Warnick, C. Salvaggio, and J. R. Schott, "Resolution enhancement of multispectral image data to improve classification accuracy," Photogramm. Eng. Remote Sens., vol. 59, no. 1, pp. 67–72, 1993.

2. J. Nunez, X. Otazu, O. Fors, A. Prades, V. Pala, and R. Arbiol, "Multiresolution- based image fusion with addtive wavelet decomposion," IEEETrans. Geosci. Remote Sens., vol. 37, no. 3, pp. 1204–1211, May 1999.

3. E. J. Candès, "Harmonic analysis of neural networks," Appl. Comput. Harmon. Anal., vol. 6, pp. 197–218, 1999.

4. E. J. Candès and D. L. Donoho, "Curvelets—A surprisingly effectivenonadaptive representation for objects with edges," in Curve and Surface Fitting: Saint-Malo, A. Cohen, C. Rabut, and L. L. Schumaker, Eds. Nashville, TN: Vanderbilt Univ. Press, 1999.

5. J. L. Starck, E. J. Candès, and D. L. Donoho, "The curvelet transform for image denosing," IEEE Trans. Image Process., vol. 11, no. 6, pp. 670–684, Jun. 2002.

6. "Gray and color image contrast enhancement by the curvelet transform," IEEE Trans. Image Process., vol. 12, no. 6, pp. 706–717, Jun. 2003.

7. T. Ranchin, B. Aiazzi, L. Alparone, S. Baronti, and L. Wald, "Image fusion—The ARSIS concept and some successful implementation schemes," ISPRS J. Photogramm. Remote Sens., vol. 58, pp. 4–18, 2003.

8. T. Ranchin and L. Wald, "Fusion of high spatial and spectral resolution images: The ARSIS concept and its implementation," Photogramm. Eng. Remote Sens., vol. 66, pp. 49–61, 2000.

9. L. Wald, T. Ranchin, and M. Mangolini, "Fusion of satellite images of different spatial resolution: Assessing the quality of resulting images," Photogramm. Eng. Remote Sens., vol. 63, no. 6, pp. 691–699, 1997.

10. M. González-Audícana, J. L. Saleta, R. G. Catalán, and R. García, "Fusion of multispectral and panchromatic images using improved IHS and PCA mergers based on wavelet decomposition," IEEE Trans. Geosci. Remote Sens., vol. 42, no. 6, pp. 1291–1299, Jun. 2004.

11. Y. Chibani and A. Houacine, "The joint use of IHS transform and redundant wavelet decomposition for fusing multispectral and panchromatic images," Int. J. Remote Sens., vol. 23, no. 18, pp. 3821–3833, 2002.

12. J. Zhou, D. L. Civco, and J. A. Silander, "A wavelet transform method to merge Landsat TM and SPOT panchromatic data," Int. J. Remote Sens., vol. 19, no. 4, pp. 743–757, 1998.

13. Heiko Hirschmüller, "Stereo processing by semi-global matching and mutual information," IEEE Transactions on Pattern Analysis and Machine Intelligence, vol. 30, no. 2, pp. 328–341, 02 2008.

14. Pablo d'Angelo and Peter Reinartz, "Semiglobal matching results on the isprs stereo matching benchmark," Proceedings ISPRS Hannover Workshop 2011: High Resolution Earth Imaging for Geospatial Information, 2011.

15. Li Zhang and Armin Gruen, "Multi-image matching for dsm generation from ikonos imagery," ISPRS Journal of Photogrammetry and Remote Sensing, vol. 60, no. 3, pp. 195–211, 2006.

16. S.M. Seitz, B. Curless, J. Diebel, D. Scharstein, and R. Szeliski, "A comparison and evaluation of multi-view stereo reconstruction algorithms," in Computer Vision and Pattern Recognition, 2006 IEEE Computer Society Conference on, june 2006, vol. 1, pp. 519–528.

17. George Vogiatzis, Carlos Hernandez Esteban, Philip H. S. Torr, and Roberto Cipolla, "Multiview stereo via volumetric graph-cuts and occlusion robust photo consistency," IEEE Transactions on Pattern Analysis and Machine Intelligence, vol. 29, pp. 2241–2246, 2007.

18. Y. Furukawa and J. Ponce, "Accurate, dense, and robust multiview stereopsis," Pattern Analysis and Machine Intelligence, IEEE Transactions on, vol. 32, no. 8, pp. 1362–1376, aug. 2010.

19. Ramin Zabih and John Woodfill, "Non-parametric local transforms for computing visual correspondence," in ECCV '94: Proceedings of the Third European Conference-Volume II on Computer Vision, London, UK, 1994, pp. 151–158, Springer-Verlag.

20. H. Hirschmüller and D. Scharstein, "Evaluation of stereo matching costs on image with radiometric differences," IEEE Transactions on Pattern Analysis and Machine Intelligence, vol. 31, no. 9, pp. 1582–1599, 2009.

21. K. Sarada, V. Lakshman Narayana, (2020), "Improving Relevant Text Extraction Accuracy using Clustering Methods", TEST Engineering and Management, Volume 83, Page Number: 15212–15219.

22. K. Sarada, V. Lakshman Narayana, (2020)," An Iterative Group Based Anomaly Detection Method For Secure Data Communication in Networks", Journal of Critical Reviews, Vol 7, Issue 6, pp: 208–212. doi: 10.31838/jcr.07.06.39.

23. Banavathu Mounika, P. Anusha, V. Lakshman Narayana, (2020), " Use of Block Chain Technology In Providing Security During Data Sharing", Journal of Critical Reviews, Vol 7, Issue 6, pp: 338–343. doi: 10.31838/jcr.07.06.59.

24. V. Lakshman Narayana, B. Naga Sudheer,(2020)," Fuzzy Base Artificial Neural Network Model For Text Extraction From Images", Journal of Critical Reviews, Vol 7, Issue 6, pp: 350–354, doi: 10.31838/jcr.07.06.61.

25. V. Lakshman Narayana, A. Peda Gopi, (2020)," Accurate Identification And Detection Of Outliers In Networks Using Group Random Forest Methodoly", Journal of Critical Reviews, Vol 7, Issue 6, pp: 381–384, doi: 10.31838/jcr.07.06.67.

26. Sandhya Pasala, V. Pavani, G. Vidya Lakshmi, V. Lakshman Narayana, (2020)," Identification Of Attackers Using Blockchain Transactions Using Cryptography Methods", Journal of Critical Reviews, Vol 7, Issue 6, pp: 368–375, doi: 10.31838/jcr.07.06.65

27. C. R. Bharathi, Vejendla. Lakshman Narayana , L. V. Ramesh, (2020)," Secure Data Communication Using Internet of Things", International Journal of Scientific & Technology Research, Volume 9, Issue 04, pp: 3516–3520.

28. J. Grodecki, G. Dial, and J. Lutes, "Mathematical model for 3D feature extraction from multiple satellite images described by RPCs," in ASPRS Annual Conf. Proc., 2004.